

# Disease- and Treatment-related Complication on F-18-Fluorodeoxyglucose Positron Emission Tomography/Computed Tomography in Oncology Practice: A Pictorial Review

## Abstract

F-18-fluorodeoxyglucose positron emission tomography/computed tomography (PET/CT) is routinely performed in oncology patients for various indications including staging, restaging, recurrence detection, and treatment response evaluation. Many disease- and treatment-related complications can be incidentally detected on PET/CT, which may be due to the complication of radiotherapy, chemotherapy, intervention, or primary tumor itself. Some of these complications could be life threatening and need urgent intervention. Therefore, these incidental findings should be recognized on PET/CT and immediately informed to the treating physicians if required urgent intervention.

**Keywords:** Chemotherapy related, complication, F-18-fluorodeoxyglucose, oncology, positron emission tomography/computed tomography, radiation induced

## Introduction

F-18-fluorodeoxyglucose (FDG) positron emission tomography/computed tomography (PET/CT) is routinely performed in oncology patients now-a-days for various indications including staging, restaging, recurrence detection, and therapeutic response evaluation. Many disease- and treatment-related complications can be incidentally detected on PET/CT, which may be due to the complication of radiotherapy, chemotherapy, intervention, or primary tumor itself. These complications could be life threatening and sometimes need urgent intervention. Therefore, it should be recognized on PET/CT study and immediately informed to the treating physicians if required urgent intervention. In this review article, we describe some of the rarely seen complication in cancer patients during FDG PET/CT studies.

## Nervous System

### Mass effect

Any intra- or extra-axial lesion in the brain causes mass effect on the brain parenchyma. This leads to midline shift (MLS) in the brain, which is one of the indicators of increased intracranial pressure [Figure 1]. Brain MLS is a potentially life-threatening condition and

requires urgent management. MLS is also a quantitative measure of mass effect or the degree of compression.<sup>[1]</sup> The midline of the brain is assumed to be coplanar with falx cerebri - MLS may be associated with other signs of raised intracranial pressure, for example, hydrocephalus and herniation and should be given due attention while reporting PET/CT studies.

### Spinal cord compression/nerve compression

The spinal cord compression could be due to benign conditions (intervertebral disc protrusion, trauma, tuberculosis, fractures, and benign tumors) or malignant etiologies (vertebral metastasis and compression by primary tumors). This is a surgical emergency and requires prompt intervention to prevent permanent neurological deficit. Patients may present with pain, signs of neurological deficit, and urinary retention. CT scan is not much helpful in assessing cord compression. However, in advance disease, CT studies may show cord compression [Figure 2] and a magnetic resonance (MR) study is usually recommended which is the imaging modality of choice to assess spinal cord pathology. Evaluation of spinal canal for extension of soft-tissue component of tumors within and evidence of nerve root

**Raghava Kashyap,  
Kanhaiyalal  
Agrawal<sup>1</sup>,  
Harmandeep Singh<sup>2</sup>,  
Bhagwant Rai  
Mittal<sup>2</sup>**

*Department of Nuclear Medicine and Positron Emission Tomography, Mahatma Gandhi Cancer Hospital, Visakhapatnam, Andhra Pradesh, <sup>1</sup>Department of Nuclear Medicine, All India Institute of Medical Sciences, Bhubaneswar, Odisha, <sup>2</sup>Department of Nuclear Medicine and Positron Emission Tomography, Postgraduate Institute of Medical Education and Research, Chandigarh, India*

### Address for correspondence:

*Dr. Kanhaiyalal Agrawal,  
Department of Nuclear Medicine, All India Institute of Medical Sciences, Bhubaneswar - 751 019, Odisha, India.  
E-mail: drkanis@gmail.com*

### Access this article online

**Website:** www.ijnm.in

**DOI:** 10.4103/ijnm.IJNM\_78\_17

### Quick Response Code:



**How to cite this article:** Kashyap R, Agrawal K, Singh H, Mittal BR. Disease- and treatment-related complication on F-18-fluorodeoxyglucose positron emission tomography/computed tomography in oncology practice: A pictorial review. Indian J Nucl Med 2017;32:304-15.

This is an open access article distributed under the terms of the Creative Commons Attribution-NonCommercial-ShareAlike 3.0 License, which allows others to remix, tweak, and build upon the work non-commercially, as long as the author is credited and the new creations are licensed under the identical terms.

For reprints contact: reprints@medknow.com

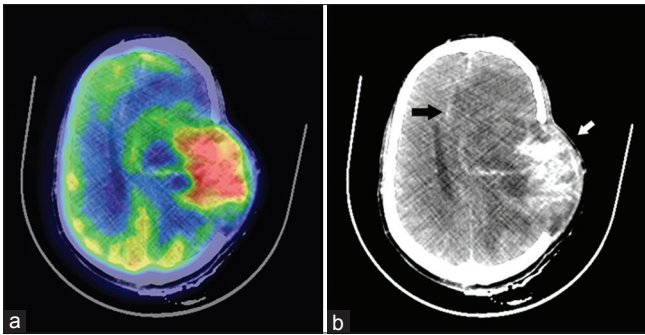


**Figure 1:** Large intensely hypermetabolic (a) glioblastoma multiforme (b, white arrow) on F-18-fluorodeoxyglucose positron emission tomography/computed tomography study showing significant perilesional edema, mass effect, and midline shift toward the right side (b, black arrow). Status post-craniotomy to relieve the intracranial pressure noted

compression in the form of neural foramina involvement needs to be reported. Multiplanar reconstruction and review of sagittal and coronal views may better aid in the evaluation of PET/CT images for cord/nerve compression.

## Lungs

### Radiation-induced lung disease

Radiation-induced lung disease (RILD) is common after radiotherapy for chest wall and intrathoracic malignancies. CT scan usually shows ground glass opacities or air space consolidation in the acute phase and traction bronchiectasis, volume loss, or consolidation in the late phase following conventional radiotherapy to the chest [Figure 3].<sup>[2]</sup> Recent advances in radiation therapy, i.e., intensity-modulated radiotherapy, image-guided radiotherapy, and stereotactic body radiotherapy (SBRT) help in delivering higher radiation dose to tumors while reducing unnecessary doses to surrounding normal tissue.<sup>[3]</sup> These techniques produce atypical radiologic manifestations of RILD. It is essential to differentiate RILD from local residual/recurrence disease in the lung or infection. FDG PET/CT is useful in differentiating metabolically active tumor from inactive fibrosis after radiation therapy. However, FDG PET/CT frequently shows false-positive tracer uptake due to radiation pneumonitis if performed immediately after the completion of radiation therapy [Figure 3].<sup>[4]</sup> Therefore, to avoid false-positive results, FDG PET/CT is not advisable until at least 3 months after the completion of radiation therapy. Review of baseline/pretreatment images yields important information to differentiate areas of disease involvement and post-treatment changes [Figure 3a].

### Pulmonary thrombosis

Pulmonary thromboembolism (PTE) is the third most common acute cardiovascular disease.<sup>[5]</sup> Oncology patients are prone to the development of venous thromboembolism because of underlying hypercoagulable state. Cancer patients with PTE usually present with atypical clinical presentations and may be asymptomatic. Incidental PTE

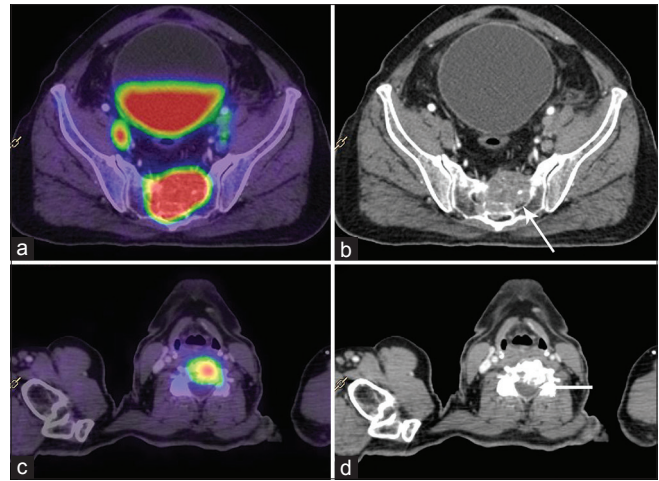


**Figure 2:** F-18-fluorodeoxyglucose positron emission tomography/computed tomography study in a 68-year-old male patient with unknown primary and suspicious metastatic lesions in the spine showed primary in the prostate (not shown here). Images show intensely hypermetabolic lesion in the sacrum (a) which on computed tomography images shows compromise of neural foramina (arrow in b). The day following positron emission tomography scan, the patient developed paraparesis with ventilator dependence for respiration. (c) Hypermetabolic lesion in C5 vertebral body extending into and indenting the spinal canal with cord compression (d arrow) which was worsened by ambulation of the patient

on contrast-enhanced computed tomography (CECT) studies in the oncologic population is noted in 0.58%–4.0% of patients.<sup>[6]</sup> CT findings show an intraluminal filling defect in the involved pulmonary artery and its branches. F-18 FDG PET/CT is now a standard imaging modality in various malignancies. Many centers perform contrast CT protocol during routine F-18 FDG PET/CT procedure. Hypermetabolism in the lumen of pulmonary artery [Figure 4], four-chamber cardiac uptake, and the presence of a rim of hypermetabolism surrounding a pulmonary infarction are various PET findings associated with PTE.<sup>[6]</sup> Differential diagnosis of intraluminal pulmonary artery hypermetabolism is pulmonary artery sarcoma and pulmonary artery metastasis.<sup>[7,8]</sup> However, there is a low-grade tracer uptake in PTE, whereas much higher metabolism is reported for pulmonary artery malignancies and tumor emboli. Although primary mechanism for tracer uptake in the PTE is uncertain, it can be due to inflammatory cells that constitute the pulmonary embolus.<sup>[5]</sup>

### Aspiration

Swallowing dysfunction and dysphagia are frequent morbidities in cancers of the head and neck and esophagus. Luminal narrowing from the tumor as well as post-surgical and radiation side effects are the contributory factors. Swallowing dysfunction leads to aspiration of food into the lungs and secondary pneumonitis. Aspiration pneumonia is associated with increased risk of mortality in these patients. Aspiration presents as consolidation, patchy ground glass changes, or tree-in-bud appearances. On F-18 FDG PET/CT, relative low metabolic activity

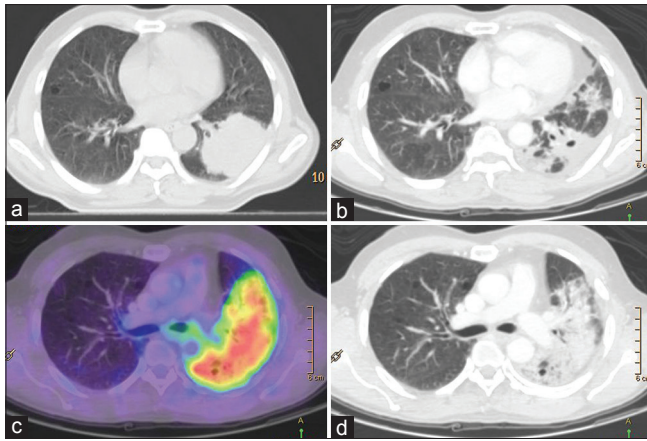


**Figure 3:** (a) Computed tomography study of a patient with the left lung mass before radiation while (b) shows a significant resolution in the lesion post radiotherapy. (c) Intense metabolic activity on F-18-fluorodeoxyglucose positron emission tomography corresponding to consolidation-like changes on computed tomography images (d) in the upper lobe of the left lung post radiation, likely due to radiation induced lung disease

along with diffuse pattern of involvement suggests possible inflammatory nature in these cases in addition to the changes noticed on CT [Figure 5].

### Bronchopleural fistula

In oncology patients, cavitory lesions in the lungs are seen due to several etiologies, for example, primary bronchogenic carcinoma, pulmonary metastasis, infections, etc. Squamous cell carcinoma is the most common cause composing 69% of total cavitating lung metastases.<sup>[9]</sup> In addition, metastatic adenocarcinoma and sarcoma can also cavitate.<sup>[9]</sup> The exact mechanism of cavitation within a lung metastasis is not known, but it has been hypothesized that cavitation could be either due to tumor necrosis or a check-valve mechanism that develops by means of tumor infiltration into the bronchial structure.<sup>[10,11]</sup> In general, cavitating metastases have a thick and irregular wall, but thin-walled cavities can be seen usually with metastases from sarcomas and adenocarcinomas.<sup>[9]</sup>

Spontaneous pneumothorax is a rare manifestation of metastasis in the lung.<sup>[12]</sup> Rarely, necrosis of subpleurally located metastases may lead to formation of bronchopleural fistula resulting in pneumothorax [Figure 6]. In some situation, these subpleural metastases are small and not recognizable in X-rays. Thus, pneumothorax is the presenting manifestation. Pneumothorax presentation may range from completely asymptomatic to life-threatening respiratory distress. Therefore, pulmonary metastasis should be considered while evaluating the etiology of spontaneous pneumothorax in cancer patients.

### Mediastinum

#### Esophageal perforation with tracheoesophageal fistula

Esophageal perforation (EP) is a potential life-threatening medical emergency. This leads to high morbidity and

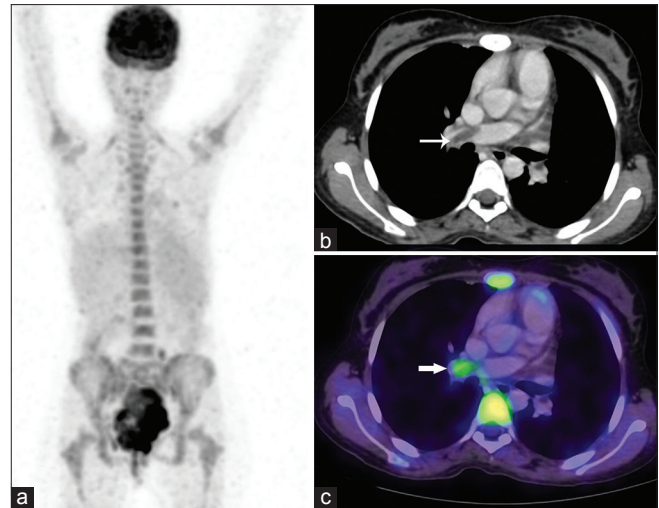


**Figure 4:** Young female patient with large sigmoid growth underwent F-18-fluorodeoxyglucose positron emission tomography/computed tomography scan (a) for staging showed a filling defect in the right pulmonary artery on computed tomography images (arrow b) which was metabolically active (arrow c). The presence of metabolic activity in pulmonary thrombus should raise the suspicion of tumor thrombus

mortality rate (at least 20%).<sup>[13]</sup> EP is usually iatrogenic, mainly due to endoscopic procedures. However, it could be spontaneous or due to trauma. Perforation in the esophageal cancer could be iatrogenic resulting from dilatation of the narrowed esophagus, radiotherapy related or due to advanced stage of progressive esophageal carcinoma.<sup>[14]</sup> Symptoms and signs of EP are variable and non-specific in many patients. A missed diagnosis and first diagnosis at autopsy are described in 17% of cases.<sup>[15]</sup> In general, patients present with acute- and sudden-onset chest pain radiating to the back or to the left shoulder. Typical signs and symptoms of EP are vomiting, chest pain, and subcutaneous emphysema (Mackler triad).<sup>[16]</sup> Further symptoms are related to the site of esophagus perforated, for example, neck pain in patients with perforation of cervical esophagus and acute abdominal or epigastric pain in those with gastroesophageal junction perforation.<sup>[13]</sup> CT study in EP usually shows thickened esophageal wall, contrast material extravasation, focal esophageal wall defect, periesophageal air and fluid collections, mediastinal inflammation, mediastinal fluid collection, and pleural effusion.<sup>[17]</sup> Rarely, tracheoesophageal fistula (TEF) develops in patients with esophageal cancer [Figure 7]. Malignant TEF may be seen in association with other malignancies, such as lung cancer, tracheal cancer, and Hodgkin's disease.<sup>[18]</sup> The incidence of TEF in patients with esophageal cancer ranges from 5% to 10%.<sup>[19]</sup> The management of malignant TEF is always challenging and carries poor prognosis. The esophageal contents spill into the lungs and death is often due to respiratory infection rather than the malignancy itself.<sup>[19]</sup> F-18 FDG PET/CT may show hypermetabolism in the lungs due to infection and should not be confused with metastatic disease.



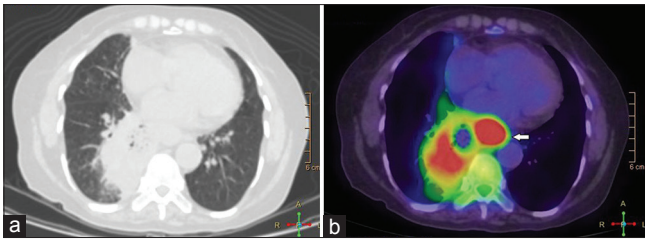


**Figure 5:** F-18-fluorodeoxyglucose positron emission tomography/computed tomography study of a patient with carcinoma esophagus post neoadjuvant chemotherapy shows residual primary (b, arrow) while the medial basal segment of the lung shows mass with central air pockets and surrounding ground glass changes (a) suggestive of aspiration. This was not noticed in the baseline positron emission tomography scan before chemotherapy. This was later confirmed due to trachea-esophageal fistula on endoscopy and stenting was done

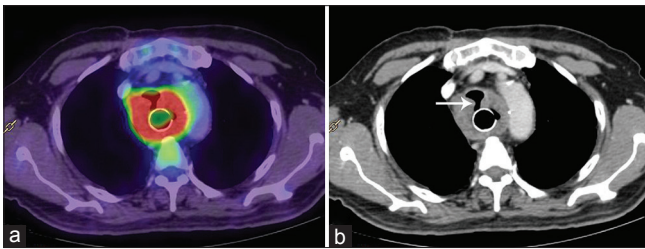


**Figure 7:** F-18-fluorodeoxyglucose positron emission tomography/computed tomography study of a patient with carcinoma esophagus showing intense tracer uptake in the primary tumor (a), which is encasing the trachea with formation of trachea-esophageal fistula (arrow in b). A self-expanding metallic stent is noted in the esophagus

### Superior vena cava syndrome

Superior vena cava syndrome (SVCS) occurs due to major vessel compression in the superior mediastinum and is a potentially life-threatening condition. There is impairment in the venous drainage of the head, neck, and upper extremities. Clinical signs and symptoms include swelling of the face, neck, and arms, distended neck veins, headache, dyspnea, coughing, and in severe cases, stridor and altered mental status. Symptoms are often exacerbated by lying down or bending forward. In SVCS, on bilateral arm elevation, there is development of facial plethora, inspiratory stridor, and non-pulsatile jugular venous pressure elevation, known as Pemberton's sign. Malignant tumors such as lung cancer, lymphoma, malignant thymoma, germ cell tumors, and metastases are responsible for the majority of SVCS cases. Lung cancer accounts for 85% of all cases of SVCS with malignant etiology.<sup>[20]</sup> Other causes of SVCS include aortic aneurysm, thyromegaly, fibrosing mediastinitis from prior irradiation, or histoplasmosis and thrombosis due to central venous access.<sup>[20]</sup> In the superior vena cava (SVC) obstruction, CT study typically shows a lack of opacification of the SVC, an intraluminal filling defect or severe narrowing of the SVC, and visualization of collateral vessels [Figure 8].<sup>[21]</sup> In general, network of smaller venous plexuses connecting the venous drainage of upper extremities is not opacified on contrast CT. Furthermore, azygos and hemiazygos

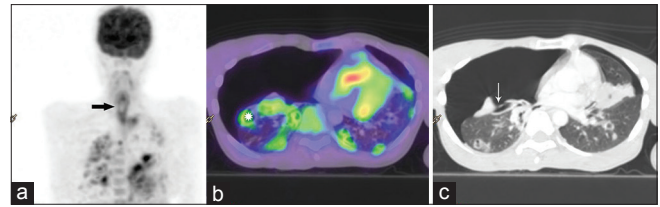


**Figure 6:** Post cricoid carcinoma, post radiotherapy, on F-18-fluorodeoxyglucose positron emission tomography/computed tomography scan showing persistent activity in the neck at the site of primary (arrow a) corresponding to stricture on endoscopy suggestive of recurrent disease. Multiple lung lesions with increased metabolism and cavity changes confirmed later as metastases (\* b). (c) Demonstrating fistula between the bronchus and pleura resulting in large right pneumothorax pushing the mediastinum to left and collapse of the lung (tension pneumothorax)

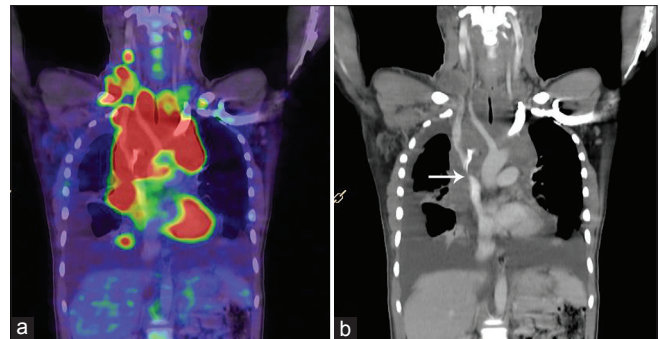


**Figure 8:** A patient with Hodgkin's disease underwent F-18-fluorodeoxyglucose positron emission tomography/computed tomography study for staging. The images show lack of opacification in part of superior vena cava (arrow in b) due to encasement by the large hypermetabolic mediastinal lymph nodal mass (a), suggestive of superior vena cava syndrome. Incidental note is also made of tracheal stenosis caused by the mass (b)

systems are also dilated. In SVC obstruction, venous flow diverts into a network of thoracic and abdominal collateral channels. The presence of collateral vessels on CT study has a sensitivity of 96% and a specificity of 92% in SVCS.<sup>[21]</sup> Although gold standard for evaluation of SVC is venogram, multidetector computed tomography provides helpful information such as the level and degree of SVC obstruction, the length of the affected segment, and detects any intraluminal clot. Treatment of SVCS depends on the etiology. In most of the cases where SVCS is due to cancer, treatment related to cancer is choice. Sometimes, patients may need endovascular stents. Therefore, timely recognition of SVC obstruction on PET/CT is essential.

### Abdomen and Pelvis

#### Intussusception

Intussusception is defined as invagination of one segment of bowel loop with its mesenteric fold (intussusceptum) into the lumen of a contiguous portion of bowel (intussusciens) as a result of peristalsis.<sup>[22]</sup> It is more common in children. Intussusception is rare in adults constituting only 5% of all intussusceptions.<sup>[22]</sup>

Intussusception could be with a lead point or without a lead point. In children, no lead point is identified in about 90% of cases and etiology is thought to enlarge lymphoid tissue following an infection. However, a lead point is seen in infants and adults in approximately 90% of cases.<sup>[23]</sup> In adults, lead points are mostly due to gastrointestinal malignancies such as colorectal carcinoma, lymphoma, and metastases.<sup>[23]</sup> Intussusception without a lead point may present as vague abdominal pain without bowel obstruction and mostly discovered incidentally on CT studies. On CT abdomen, it appears as target-like or sausage-shaped mass depending on the axial slice projection [Figure 9]. Intussusception with a lead point presents with atypical findings and often there are symptoms of partial bowel obstruction such as intermittent abdominal pain, nausea, and vomiting. On CT study, it appears as an abnormal target-like mass with cross-sectional diameter greater than that of the normal bowel. There may be associated with proximal bowel obstruction.<sup>[22]</sup> However, impaired circulation of the mesenteric vessels leading to bowel wall edema and thickened bowel loops makes it difficult to differentiate a lead mass from inflammation in the bowel loops. FDG PET/CT performed in oncology patients may sometime reveal intussusception incidentally. FDG uptake in intussusception depends on the etiology. Intense uptake has been described at the site of intussusception due to lymphoma or other malignancies.<sup>[24-27]</sup> However, intensity of FDG uptake varies in intussusception due to benign causes and possibly depends on the degree of edema and inflammation. In children, intussusceptions can be treated by enema reduction or laparoscopic approach in most of the cases. However, laparotomy is usually required in adults as in most cases, a lead point requiring treatment is present. Delay in diagnosis may lead to devastating results, including bowel infarction, perforation, peritonitis, or even death. Therefore, it is essential to recognize this potentially life-threatening condition on PET/CT.

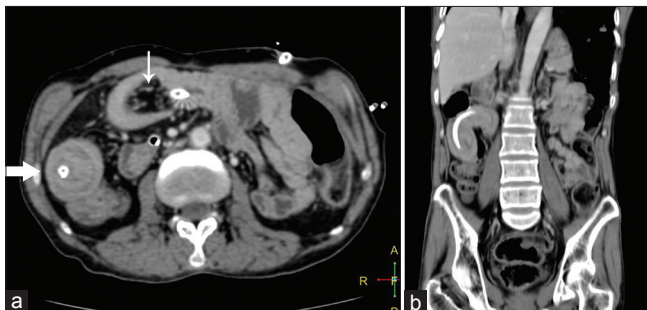


**Figure 9:** Computed tomography images showing classical target appearance of intussusception (jejunojejunal), noticed incidentally in a patient with recurrent post cricoid carcinoma (a block arrow). Further, mesenteric fold inside the jejunal loop is noted (a vertical arrow). (b) Both the intussusceptum and intussusciens in coronal plane, possibly induced by feeding jejunostomy tube noticed at the level of intussusception in the image. No abnormal metabolic activity was seen on fluorodeoxyglucose positron emission tomography at this site to suggest malignant involvement

## Bowel obstruction

Obstruction of the intestines is a common complication in patients with malignancies and needs to be recognized. It has a significant impact on the prognosis and outcomes of the patients. Mechanical as well as functional factors play a role in culmination of bowel obstruction. Causes can also be related directly to the tumor or as a consequence of the treatment administered. Functional causes include neuropathy from tumor involvement, paraneoplastic neuropathy, diabetic neuropathy, use of opioids, dehydration, and electrolyte disturbances.

Mechanical causes related to the tumor directly could be due to extrinsic compression and intramural occlusion. Treatment related causes include post-surgical adhesions or post-radiation fibrosis. International consensus definition criteria for malignant bowel obstruction include (1) clinical evidence of bowel obstruction, (b) obstruction distal to the Treitz ligament, (c) the presence of primary intra- or extra-abdominal cancer with peritoneal involvement, and (d) the absence of reasonable possibilities for a cure. Obstruction can be partial or complete. Few cases show spontaneous resolution.

The radiological signs of distension of the intestinal loops, fluid retention, air-fluid levels in the zone proximal to the occlusion as well as collapsed distal bowel segments help in recognition of the phenomenon [Figure 10]. Additional role of F-18 FDG PET/CT would be to determine unifocal versus multifocal peritoneal disease and thereby aiding treatment-related decisions.

## Hydronephrosis

Hydronephrosis (HDN) is defined as distention of the renal calyces and pelvis with urine as a result of outflow obstruction distal to the renal pelvis. HDN can be seen in patients with urogenital, retroperitoneal, and pelvic tumors and periureteral metastasis compressing the ureter. Pathology in urinary bladder, prostate, or urethra usually

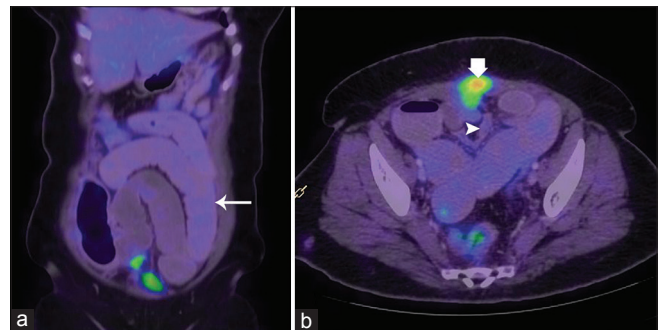


**Figure 10:** A 40-year-old female with endometrial carcinoma, post hysterectomy and radiotherapy, underwent F-18-fluorodeoxyglucose positron emission tomography/computed tomography study to rule out local recurrence. The image shows dilated small bowel loops (a arrow). Parietal wall deposit noticed (b) (bold arrow) is the culprit lesion resulting in adhesion and obstruction of proximal small bowel loops with collapse of distal loops (arrow head)



causes bilateral HDN. CT component of PET/CT generally shows thinned out cortex with dilated pelvicalyceal system [Figure 11]. CT grading system of HDN is as follows: grade 1, pelvic dilatation only; Grade 2, pelvic dilatation plus mild calyx dilation; Grade 3, severe calyx dilation; and Grade 4, calyx dilation with parenchymal thinning or atrophy.<sup>[28]</sup> CT scan also helps in ruling out other causes of HDN, e.g. calculus. F-18 FDG is mostly excreted through kidneys. The patterns of F-18-FDG excretion through HDN kidneys depend on hydration, severity of HDN, and time after which PET acquisition is done. Recognition and reporting of HDN due to malignant obstruction is essential as bilateral obstruction is a medical emergency and may lead to acute renal failure. Second, malignant obstruction of ureter is a sign of poor prognosis due to high rates of stent failure, and the reported median survival period is 4–15 months.<sup>[29-31]</sup>

### Hemorrhagic cystitis

Hemorrhagic cystitis (HC) is defined as diffuse bladder mucosal bleeding.<sup>[32]</sup> HC is a rare but serious disease that may affect patients after pelvic radiation therapy or systemic chemotherapy like cyclophosphamide.<sup>[32]</sup> Other causes of HC are bacterial, viral, fungal, and parasitic infections, some medications, and idiopathic etiology. Radiation-induced cystitis can occur as early as 6 months to as late as two decades after radiation treatment. At least 5% of patients treated with radiation therapy are expected to develop radiation cystitis.<sup>[33]</sup> Occurrence of radiation-induced HC depends on the volume of tissue treated, total radiation dose to bladder, radiotherapy fractionation, mode of delivery (external beam or brachytherapy), concurrent treatments, and radiosensitivity of the affected bladder tissue.<sup>[34]</sup> Radiotherapy alone or combined with chemotherapy causes HC directly due to bladder toxicity or indirectly causing immune suppression.<sup>[35]</sup> There is considerable variability in presentation and severity of disease. While some patients only have mild irritative symptoms with microscopic hematuria, others present with severe lower urinary tract symptoms, obstruction, urinary

retention, or life-threatening hemorrhage. Clinical features of HC are usually non-specific and may overlap with symptoms of urinary bladder infection or malignancy. In HC, FDG PET study may show false-positive intense tracer uptake in the urinary bladder [Figure 12].<sup>[36]</sup> CT component of PET/CT study may be helpful in raising suspicion and usually shows thickening of the bladder wall, intraluminal soft-tissue mass (clot), and marked inflammation in the adjacent fat.

### Urethral stricture

Urethral stricture is a late and rare complication of radiation treatment in pelvic malignancy.<sup>[37]</sup> The narrowing can occur at any location along the urethra; however, bulbomembranous stenosis accounts for approximately 90% of reported strictures after radiotherapy.<sup>[38]</sup> The overall incidence of radiation-induced urethral stricture is dependent on the dose and type of radiation.<sup>[38]</sup> Patients with radiation-induced urethral stricture present with bladder outlet obstruction. The obstructive symptoms develop gradually and progressively over months.<sup>[39]</sup> The basic diagnostic work-up includes a detailed clinical history, physical examination, urine analysis, and culture. Retrograde urethrogram and voiding cystourethrography are essential to evaluate the location and extent of the stricture.<sup>[39]</sup> However, urethral stricture may be detected incidentally on CT, MR, or PET/CT studies when performed to detect tumor recurrence. Usually, imaging findings of bladder outlet obstruction with hydroureters raise the suspicion of urethral stricture in a patient after radiation therapy [Figure 13].

### Varicocele

Varicocele is the dilatation of pampiniform plexus of veins, which is a network of small veins in the spermatic cord. A patient with varicocele may remain asymptomatic or presents with scrotal mass or swelling, scrotal pain, testicular atrophy, or infertility. A varicocele could be due

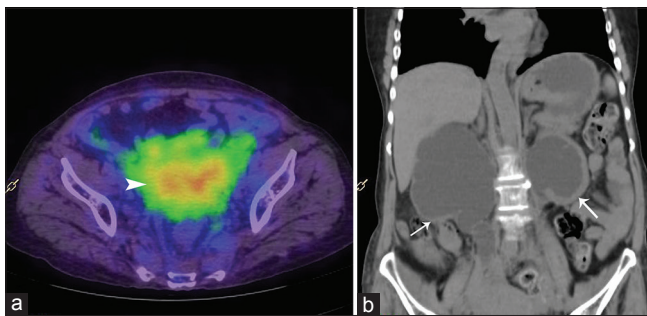


Figure 11: Staging F-18-fluorodeoxyglucose positron emission tomography/computed tomography study of a 55-year-old female patient with cervical carcinoma demonstrating the large primary with extension into the parametrium (a arrow head) resulting in compression of the ureters on both sides and gross hydronephrosis proximally with thinned out renal cortex (b arrows)

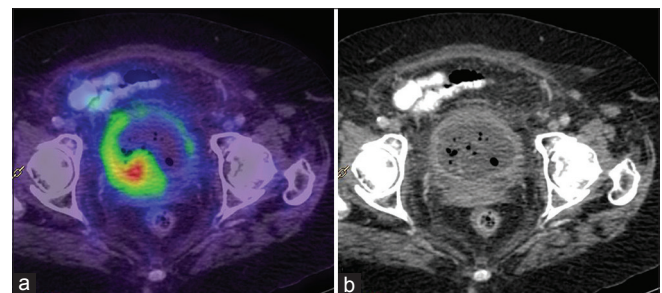
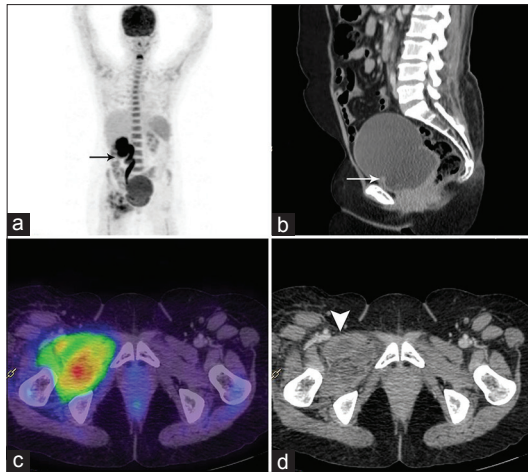


Figure 12: A 65-year-old female with a history of radiation therapy for cervical carcinoma 16 years back presented with recent onset of urinary incontinence. Local examination showed obliterated vagina and bleeding on touch. Cystoscopy showed hemorrhage which was evacuated. Clinical diagnosis of hemorrhagic cystitis was made. F-18-fluorodeoxyglucose positron emission tomography/computed tomography showed thickened wall of the urinary bladder (b) with diffuse increased uptake (a) and extensive peri-vesical stranding (b). Air shadows in the lumen are due to partially evacuated thrombi (b). No hypermetabolism to suggest local recurrence is noticed in the cervix



**Figure 13:** A patient with vault carcinoma post radiotherapy. Fluorodeoxyglucose positron emission tomography (a) shows gross right hydronephrosis (arrow). (b) Large diverticulum in the urinary bladder (arrow). Bladder outlet obstruction with bilateral hydronephrosis raised suspicion of urethral stenosis which was later confirmed clinically. Intense metabolic activity in the right hip muscles (c) which appear bulky and show edema on computed tomography images (d arrow head) is suggestive of myositis. Both myositis and urethral stenosis in this patient were side effects of radiation

to primary or secondary etiology. Majority of varicocele are primary and are due to congenitally absent or incompetent valves in the testicular vein. The left-side varicocele is more common than the right. Secondary varicoceles are less common in comparison to primary type. This results from compression of the testicular vein by an extrinsic mass, renal vein thrombus, or splenorenal shunting. Retroperitoneal malignancy invading the renal vein is a common cause of secondary varicocele. Large adrenal mass may compress the adjacent renal vein leading to varicocele.<sup>[40]</sup> Adrenocortical carcinoma (ACC) resulting in thrombosis of the renal vein is a rare cause of varicocele.<sup>[41]</sup> Varicocele could be an early presentation of non-functioning ACC. Ultrasound is the diagnostic modality of choice, which usually shows dilatation of pampiniform plexus veins and typically has a serpentine appearance. CECT study may show a dilated cluster of enhancing serpentine pampiniform plexus veins [Figure 14]. It is essential to establish the cause of varicocele to guide appropriate management.

## Pelvic fistulas

### *Vesicovaginal fistula*

Vesicovaginal fistula (VVF) is abnormal communication between urinary bladder and vagina. The most common cause of VVF is prolonged, obstructed labor.<sup>[42]</sup> However, in the developed countries, approximately 90% of VVF are due to accidental injury to the urinary bladder during surgery.<sup>[42]</sup> Other less common causes of VVF are pelvic malignancy [Figure 15], obstetric infections, and vaginal trauma.<sup>[42]</sup> In majority of patients, VVF presents with leakage of urine per vagina approximately 5–10 days after surgery. However, VVF after pelvic radiotherapy or due to

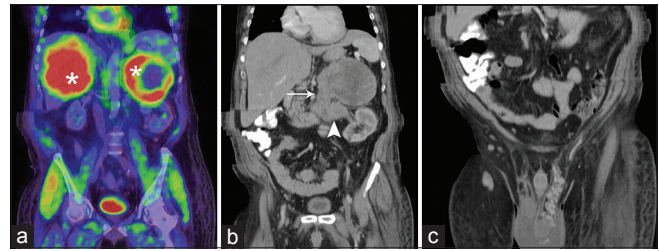


**Figure 14:** F-18-fluorodeoxyglucose positron emission tomography/computed tomography images of a patient with adrenal tumors showing intensely hypermetabolic bilateral large adrenal mass lesions with central necrosis (\*a). Extension of the tumor along the left adrenal vein (b arrow) and left renal vein (b arrow head) is also noticed resulting in secondary varicocele in the left scrotum (c)

local malignancy may present very late. Cystoscopy and vaginoscopy are often useful in diagnosis. Delayed CeCT usually shows excretion of intravenous contrast material into the vagina in approximately 60% of patients.<sup>[43]</sup> Furthermore, there may be air or fluid in the vagina. Along with these CT features, FDG PET may show accumulation of tracer in the vagina due to urine leakage.

### *Vesicouterine fistula*

Vesicouterine fistula (VUF) is rare and comprises only 4% of all urogenital fistulas.<sup>[44]</sup> The most common cause of VUF is trauma during child birth, mostly after cesarean delivery.<sup>[45]</sup> Rarely, VUF may be seen as a complication of radiation therapy and local carcinoma.<sup>[45]</sup> Symptoms depend on the level of the fistula. When VUF is present above the isthmus, the menstrual blood directly passes into the urinary bladder, leading to “Youssef’s syndrome,” i.e., amenorrhea with a patent cervical canal, periodic hematuria (menouria), and the absence of urinary leakage through the vagina.<sup>[46]</sup> When the VUF is present below the isthmus, urine leaks through the fistula from the bladder into the cervix and the vagina. Therefore, the symptoms are similar to those of the VVF.<sup>[44]</sup> When a low VUF is present, CeCT with high urinary bladder pressure is a useful imaging modality as it shows leakage of contrast material from the posterior bladder wall into the uterus [Figure 16].<sup>[43]</sup> However, when a high VUF is suspected, it is best shown on hystero-graphy.<sup>[44]</sup> In addition, CT study after hystero-graphy gives more information about the precise location of the fistulous tract.

## Musculoskeletal

### *Pathologic fractures*

Pathologic fracture refers to the bone fracture that occurs with trivial trauma due to underlying pathology in the bone. Majority of pathologic fractures in the elderly are secondary to metastatic carcinomas and multiple myeloma.<sup>[47]</sup> The most common primary malignancies that metastasize to bone are breast, lung, kidney, prostate, and thyroid carcinomas. It is well known that increased FDG uptake may be seen in both acute and subacute phases of benign fractures.<sup>[48]</sup> Further, the FDG activity may subside



as the fractures heal. FDG accumulation is likely due to migration of activated inflammatory cells in the fracture site. Similarly, increased FDG uptake is seen malignant pathologic fractures.<sup>[49]</sup> Some studies suggest that maximum standardized uptake value and medullary uptake can reliably differentiate between malignant and benign fractures, whereas other contradicts this finding.<sup>[49,50]</sup> However, in general, malignant pathologic fractures show relatively higher tracer uptake in comparison to benign fractures [Figure 17]. Further, CT findings such as soft-tissue, osteoblastic, or osteolytic lesions may help in differentiating malignant from benign fractures. It is also important to predict risk of impending fractures. Mirels proposed a scoring system based on site, nature, size of lesion, and pain. All the features are assigned scores ranging from 1 to 3. Lesion in the upper limb, lower limb, and trochanteric region is assigned score 1–3, respectively. Lesion involving  $<1/3^{\text{rd}}$ ,  $1/3^{\text{rd}}-2/3^{\text{rd}}$ , and  $>2/3^{\text{rd}}$  of the cortex is assigned score from 1 to 3, respectively. Blastic, mixed, or lytic lesion is assigned score from 1 to 3, respectively, for nature of lesion. Mild, moderate, and functional pain is assigned a score from 1 to 3, respectively. Based on an overall score, Mirels recommended prophylactic fixation for a lesion with overall score of 9 or greater, clinical judgment for overall score of 8, and radiotherapy with observation for lesions with overall score of 7 or less.<sup>[51]</sup>

### Insufficiency fractures

Insufficiency fractures are a form of stress fracture in which the physiologic load of weight-bearing causes fractures in bone that is weakened by demineralization and decreased elastic resistance.<sup>[52]</sup> Insufficiency fractures in the pelvic bones have been described following radiation therapy for gynecological, colorectal, anal, and prostate cancer.<sup>[53]</sup> It has been reported that 45%–89% of patients who receive radiation to the pelvis subsequently develop insufficiency fractures.<sup>[52]</sup> They commonly occur within 3–12 months after radiotherapy. The sacral ala adjacent to the sacroiliac joint is the most common involved site in the pelvis in addition to pubic rami adjacent to the symphysis pubis and the acetabulum.<sup>[52]</sup> Patients with insufficiency fractures may be asymptomatic or present with pain. In oncology imaging, differentiating insufficiency fractures from metastasis could be challenging and postradiation insufficiency fractures may be misinterpreted as metastases by the radiologists. Such wrong interpretation of insufficiency fractures could result in an unnecessary biopsy, which is generally not recommended as it can lead to further fracture. CT study in sacral insufficiency fractures shows linear sclerotic lesions with or without cortical discontinuity in the sacral body parallel to the sacroiliac joints. Bone scan typically demonstrates characteristic “H” or “Honda” sign in the sacrum.<sup>[54]</sup> FDG uptake in insufficiency fractures is variable and ranges from mild and diffuse to intense and heterogeneous [Figure 18]. Due to increased uptake of tracer, differentiating insufficiency fractures from new

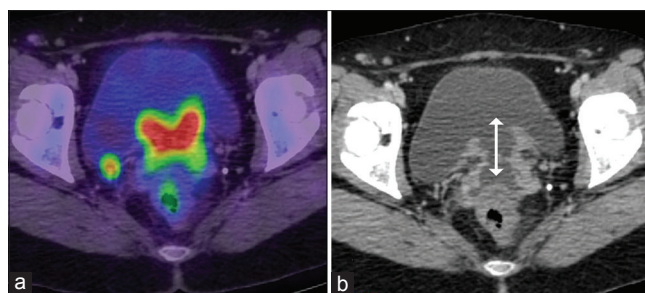


**Figure 15:** A 32-year-old female patient with a history of hysterectomy presented with vault carcinoma. Staging fluorodeoxyglucose positron emission tomography/computed tomography revealed intensely hypermetabolic mass (a) in the vault which was infiltrating into the base of the urinary bladder (double-headed arrow) (b) demonstrating vesicovaginal fistula as a direct tumor infiltration. Administration of diuretic in this case resulted in diluting the radioactive urine, thereby effectively demonstrating the metabolic activity in the lesion

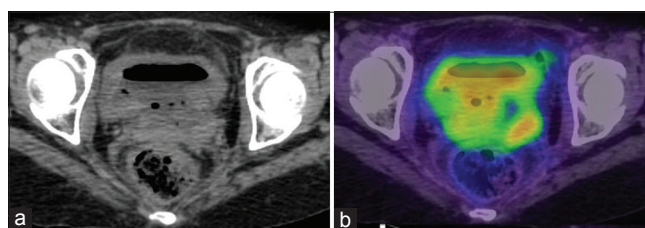


**Figure 16:** Fluorodeoxyglucose positron emission tomography/ computed tomography showing communication between uterus and urinary bladder (a, b) in a patient with recurrent cervical carcinoma post-radiation, suggestive of a uterovesical fistula

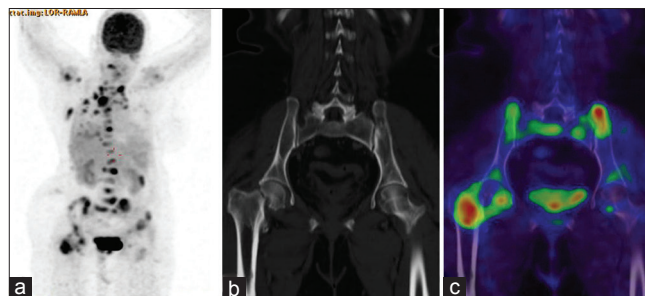


**Figure 17:** Fluorodeoxyglucose positron emission tomography/ computed tomography in a patient with non-small cell lung cancer showing multiple bone metastases (a). Pathological fracture of the neck of the right femur (b) at the site of metastases showing intense tracer uptake (c)

metastatic lesions can be challenging on FDG PET/CT. However, insufficiency fractures occur within the radiation field and sacral insufficiency fractures are usually bilateral. Furthermore, there may be typical “H” sign in the sacrum on FDG PET/CT similar to bone scintigraphy.<sup>[54]</sup> In addition, CT scan findings are helpful in such cases. In doubtful cases, serial imaging may be suggested as in insufficiency fracture, reduction in FDG uptake is noted over time.<sup>[53]</sup>

### Radiation-induced vertebral fracture

In adults, the spine is usually irradiated for metastatic disease. In these patients, postradiotherapy complication is seen in the irradiated spine. In acute phase, there may



be edema and necrosis of the bone marrow. The marrow is converted to fatty marrow as early as 2 weeks after therapy and completed by 6–8 weeks in 90% of patients.<sup>[55]</sup> Later on, osteopenia and demineralization starts, which is progressive in nature. Compression fractures of the irradiated vertebra may be seen in some patients. The incidence of vertebral compression fracture as a complication of conventional radiotherapy is <5%, whereas it ranges from 11% to 39% with SBRT.<sup>[56]</sup> The collagen in the bone gives bone ductility, increasing the tissue toughness.<sup>[56]</sup> Furthermore, collagen in bone is a crack growth inhibitor.<sup>[57]</sup> Collagen is damaged by high-dose radiation, leading to decrease bone strength. This leads to fractures in previously irradiated vertebrae. Further, metastases in the vertebra results in abnormal bone turnover and lower bone quality.<sup>[58]</sup> Therefore, time-dependent complication risk of radiotherapy for vertebral event increases with vertebral metastasis.<sup>[59]</sup> Predictive factors for vertebral fracture after radiotherapy are percentages of vertebral body tumor replacement, involvement of the posterior elements, reduced bone mineral density, and tumor location within the spine.<sup>[56]</sup> Low-grade diffuse tracer uptake is seen in the normal vertebrae on FDG PET/CT study. However, no FDG uptake is seen in the irradiated vertebra. Partially or completely collapsed vertebra on FDG PET/CT study may be noted in some patients treated with radiotherapy and should be assessed on PET only sagittal images, which show photopenic region corresponding to the irradiated collapsed vertebrae [Figure 19].

### Osteoradionecrosis

Osteoradionecrosis (ORN) is an area of non-viable bone at the site of radiotherapy. This is a serious and often debilitating complication of radiotherapy. The mandible is a common site of ORN due to tenuous blood supply.<sup>[59]</sup> The factors responsible for the development of ORN are trauma (such as dental extraction), oral hygiene, and preexisting conditions such as diabetes with amount of radiation delivered to the affected bone being the primary factor.<sup>[59,60]</sup> The incidence of mandibular ORN ranges from 2% to 22%.<sup>[61]</sup> In addition, superimposed infection may be seen in a few mandibular ORN. The earliest imaging of ORN is cortical defect. Later on, there can be trabecular disorganization, air within the bone marrow space, pathologic fracture, and fragmentation.<sup>[59]</sup> Imaging findings in patients with superimposed infection are subperiosteal abscess formation, soft-tissue abscesses and soft-tissue phlegmon. It is challenging but essential to differentiate sterile from infected ORN and between ORN and tumor recurrence. On F-18 FDG PET/CT, increased tracer uptake is seen in all three conditions [Figure 20]. Further, the intensity of uptake cannot always differentiate ORN from tumor recurrence.<sup>[60]</sup> Other differential diagnosis of increased tracer uptake in the mandible is residual disease due to previous bone involvement and benign local

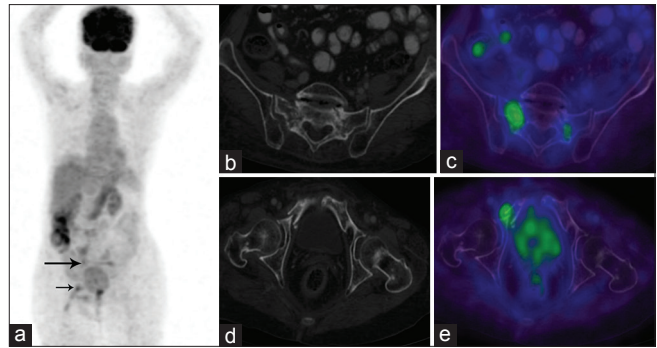


**Figure 18:** A patient with cervical carcinoma presented with severe back pain 6 months after radiation. Fluorodeoxyglucose positron emission tomography/computed tomography demonstrates fracture lines in the sacrum (b) and the pubic ramus on the right side (d) both of which show only mild metabolic activity (a arrows, c and e)

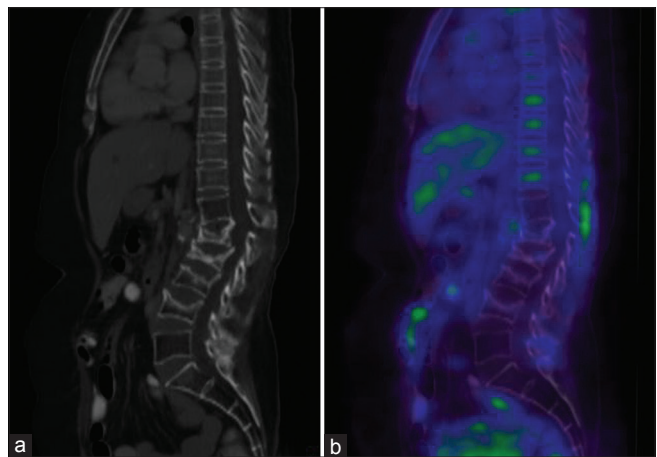


**Figure 19:** A patient with cervical carcinoma post radiotherapy. Fluorodeoxyglucose positron emission tomography/computed tomography study shows wedge collapse of the L1–L4 vertebrae (a) with no abnormal metabolic activity (b). Sharp demarcation of the physiologic metabolic activity in the spine is noticed with vertebrae above D12 showing normal tracer uptake while those below D11 which were included in radiation field show absent metabolism (b)

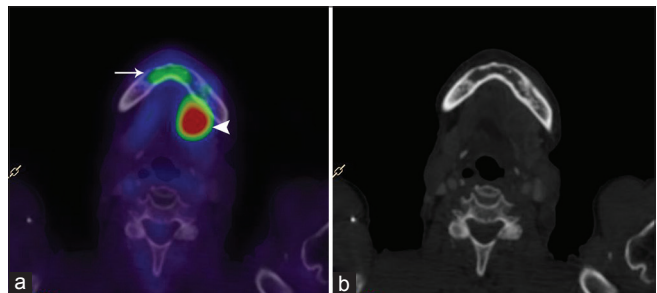


**Figure 20:** Fluorodeoxyglucose positron emission tomography/computed tomography study of a patient with tongue carcinoma, previously treated with radiotherapy 3 years back, presented with local recurrence (arrowhead a). Furthermore, noticed is mild metabolic activity in a lytic lesion (a, arrow) in the mandible in midline (b) suggestive of osteonecrosis post radiotherapy

dental infection. Therefore, CT findings should be given utmost care to avoid false positive on F-18 FDG PET/CT imaging. ORN may be associated with inflammatory changes in the surrounding soft tissues, whereas tumor

recurrence is associated with asymmetric discrete solid or cystic mass. Furthermore, bony sclerosis is more commonly seen in ORN in comparison to tumor recurrence.<sup>[60]</sup> Sestamibi scintigraphy could possibly differentiate osteonecrosis and tumor recurrence as no tracer uptake is seen in osteonecrosis in a few studies.<sup>[62]</sup>

### Radiation myositis

Radiation myositis of striated muscle is a rare complication of radiation therapy. Dose fractionation schedule is an important determinant of the radiation-induced muscle injury.<sup>[63]</sup> Furthermore, chemotherapy has potential to exacerbate tissue injury caused by radiation therapy, phenomenon known as radiation recall.<sup>[64]</sup> In such cases, previously irradiated tissue becomes more vulnerable to toxic effect of subsequent systemic therapy. Radiation recall most commonly occurs as dermatitis but could also leads to myositis, pneumonitis, or enterocolitis.<sup>[64-67]</sup> Time interval between radiation treatment and radiographic appearance of radiation-induced muscle changes have been studied with both photon and neutron therapy. MR imaging showed that muscle edema following radiation therapy with neutrons peaks at about 6 months compared to 12–18 months after treatment with photons.<sup>[63]</sup> There is also longer persistence of edema for the neutron-treated patients. Complete resolution of myositis induced by photons occurs in about half of the patients within 2–3 years, whereas time for resolution is longer in neutron-induced myositis.<sup>[63]</sup> Patients usually present with pain and restricted range of motion if joint is involved. T2-weighted MR images usually show edema in the muscles. Increased FDG uptake on PET/CT studies has been described in myositis.<sup>[68,69]</sup> Hence, it is important to identify this false-positive FDG uptake in myositis in oncology patients [Figure 13].

### Conclusion

Complications related to cancer or cancer treatment may be frequently seen in FDG PET/CT studies. Some of these conditions may be life threatening and early recognition may save patient's life. Therefore, a nuclear medicine physician should have adequate knowledge of these complications.

### Financial support and sponsorship

Nil.

### Conflicts of interest

There are no conflicts of interest.

### References

- Liao CC, Xiao F, Wong JM, Chiang IJ. Automatic recognition of midline shift on brain CT images. *Comput Biol Med* 2010;40:331-9.
- Choi YW, Munden RF, Erasmus JJ, Park KJ, Chung WK, Jeon SC, *et al.* Effects of radiation therapy on the lung: Radiologic appearances and differential diagnosis. *Radiographics* 2004;24:985-97.
- Lee P, Kupelian P, Czernin J, Ghosh P. Current concepts in F18 FDG PET/CT-based radiation therapy planning for lung cancer. *Front Oncol* 2012;2:71.
- Larici AR, del Ciello A, Maggi F, Santoro SI, Meduri B, Valentini V, *et al.* Lung abnormalities at multimodality imaging after radiation therapy for non-small cell lung cancer. *Radiographics* 2011;31:771-89.
- Wittram C, Scott JA. 18F-FDG PET of pulmonary embolism. *AJR Am J Roentgenol* 2007;189:171-6.
- Flavell RR, Behr SC, Brunsing RL, Naeger DM, Pampaloni MH. The incidence of pulmonary embolism and associated FDG-PET findings in IV contrast-enhanced PET/CT. *Acad Radiol* 2014;21:718-25.
- Ito K, Kubota K, Morooka M, Shida Y, Hasuo K, Endo H, *et al.* Diagnostic usefulness of 18F-FDG PET/CT in the differentiation of pulmonary artery sarcoma and pulmonary embolism. *Ann Nucl Med* 2009;23:671-6.
- Lee EJ, Moon SH, Choi JY, Lee KS, Choi YS, Choe YS, *et al.* Usefulness of fluorodeoxyglucose positron emission tomography in malignancy of pulmonary artery mimicking pulmonary embolism. *ANZ J Surg* 2013;83:342-7.
- Seo JB, Im JG, Goo JM, Chung MJ, Kim MY. Atypical pulmonary metastases: Spectrum of radiologic findings. *Radiographics* 2001;21:403-17.
- Dodd GD, Boyle JJ. Excavating pulmonary metastases. *Am J Roentgenol Radium Ther Nucl Med* 1961;85:277-93.
- Chaudhuri MR. Cavitary pulmonary metastases. *Thorax* 1970;49:412-6.
- Hsu JS, Chou SH, Tsai KB, Chuang MT. Lingual carcinoma metastases presenting as spontaneous pneumothorax. *J Formos Med Assoc* 2009;108:736-8.
- Søreide JA, Viste A. Esophageal perforation: Diagnostic work-up and clinical decision-making in the first 24 hours. *Scand J Trauma Resusc Emerg Med* 2011;19:66.
- Duan D, Zou J, Cai Z, Wu S, Xiao H, Zhou Y, *et al.* Surgical treatment of perforation with esophageal carcinoma. *Chin J Clin Oncol* 2006;2:126-9.
- Vidarsdottir H, Blondal S, Alfredsson H, Geirsson A, Gudbjartsson T. Oesophageal perforations in Iceland: A whole population study on incidence, aetiology and surgical outcome. *Thorac Cardiovasc Surg* 2010;58:476-80.
- Mackler SA. Spontaneous rupture of the esophagus; an experimental and clinical study. *Surg Gynecol Obstet* 1952;95:345-56.
- Young CA, Menias CO, Bhalla S, Prasad SR. CT features of esophageal emergencies. *Radiographics* 2008;28:1541-53.
- Gschossmann JM, Bonner JA, Foote RL, Shaw EG, Martenson JA Jr., Su J, *et al.* Malignant tracheoesophageal fistula in patients with esophageal cancer. *Cancer* 1993;72:1513-21.
- Sharma A, Rehman MU, Cowen ME. Management of a difficult malignant tracheoesophageal fistula. *Interact Cardiovasc Thorac Surg* 2003;2:665-7.
- Rizvi I, Zaman S, Zaidi N, Ashraf SM, Kumar A, Gupta A, *et al.* Superior vena cava syndrome caused by Hodgkin's lymphoma in an adolescent girl. *BMJ Case Rep* 2012;2012.
- Sheth S, Ebert MD, Fishman EK. Superior vena cava obstruction evaluation with MDCT. *AJR Am J Roentgenol* 2010;194:W336-46.
- Kim YH, Blake MA, Harisinghani MG, Archer-Arroyo K, Hahn PF, Pitman MB, *et al.* Adult intestinal intussusception: CT appearances and identification of a causative lead point. *Radiographics* 2006;26:733-44.



23. Choi SH, Han JK, Kim SH, Lee JM, Lee KH, Kim YJ, *et al.* Intussusception in adults: From stomach to rectum. *AJR Am J Roentgenol* 2004;183:691-8.
24. Kaminski CY, Kaminski JM, Guttentag AR, Tran H. Positron emission tomography in intussusception of colon cancer, where computed tomography failed. *Clin Nucl Med* 2003;28:60-1.
25. Slaby J, Suri U. Metastatic melanoma with multiple small bowel intussusceptions. *Clin Nucl Med* 2009;34:483-5.
26. Chamroonrat W, Cheng G, Servaes S, Zhuang H. Intussusception incidentally detected by FDG-PET/CT in a pediatric lymphoma patient. *Ann Nucl Med* 2010;24:555-8.
27. Kang HJ, Beylergil V, Price AP, Abramson SJ, Carrasquillo JA. FDG PET/CT detection of intussusception caused by lymphoma in a pediatric patient. *Clin Nucl Med* 2014;39:97-8.
28. Cho A, Chung YE, Lee JH, Yun M, Lee JD, Kang WJ, *et al.* Evaluation of 18F-FDG excretion patterns in malignant obstructive uropathy. *Clin Nucl Med* 2013;38:695-702.
29. Izumi K, Mizokami A, Maeda Y, Koh E, Namiki M. Current outcome of patients with ureteral stents for the management of malignant ureteral obstruction. *J Urol* 2011;185:556-61.
30. Parkin DM, Bray F, Ferlay J, Pisani P. Global cancer statistics, 2002. *CA Cancer J Clin* 2005;55:74-108.
31. Rosenberg BH, Bianco FJ Jr., Wood DP Jr., Triest JA. Stent-change therapy in advanced malignancies with ureteral obstruction. *J Endourol* 2005;19:63-7.
32. Alesawi AM, El-Hakim A, Zorn KC, Saad F. Radiation-induced hemorrhagic cystitis. *Curr Opin Support Palliat Care* 2014;8:235-40.
33. Smit SG, Heyns CF. Management of radiation cystitis. *Nat Rev Urol* 2010;7:206-14.
34. Zwaans BM, Nicolai HG, Chancellor MB, Lamb LE. Challenges and opportunities in radiation-induced hemorrhagic cystitis. *Rev Urol* 2016;18:57-65.
35. Johnston D, Schurtz E, Tourville E, Jones T, Boemer A, Giel D, *et al.* Risk factors associated with severity and outcomes in pediatric patients with hemorrhagic cystitis. *J Urol* 2016;195:1312-7.
36. Vicente AM, Castrejón AS, Muñoz AP, Woll PP, García AN. Impact of 18F-FDG PET/CT with retrograde filling of the urinary bladder in patients with suspected pelvic malignancies. *J Nucl Med Technol* 2010;38:128-37.
37. Viswanathan AN, Lee LJ, Eswara JR, Horowitz NS, Konstantinopoulos PA, Mirabeau-Beale KL, *et al.* Complications of pelvic radiation in patients treated for gynecologic malignancies. *Cancer* 2014;120:3870-83.
38. Khouardaji I, Parke J, Chennamsetty A, Burks F. Treatment of urethral strictures from irradiation and other nonsurgical forms of pelvic cancer treatment. *Adv Urol* 2015;2015:476390.
39. Hofer MD, Gonzalez CM. Management of radiation-induced urethral strictures. *Transl Androl Urol* 2015;4:66-71.
40. Geleit RJ, Bhardwaj R, Fish D, Sriprasad S. A unique presentation of a complex haemorrhagic adrenal pseudocyst. *BMJ Case Rep* 2016;2016.
41. Cheungpasitporn W, Horne JM, Howarth CB. Adrenocortical carcinoma presenting as varicocele and renal vein thrombosis: A case report. *J Med Case Rep* 2011;5:337.
42. Garthwaite M, Harris N. Vesicovaginal fistulae. *Indian J Urol* 2010;26:253-6.
43. Yu NC, Raman SS, Patel M, Barbaric Z. Fistulas of the genitourinary tract: A radiologic review. *Radiographics* 2004;24:1331-52.
44. Smayra T, Ghossain MA, Buy JN, Moukarzel M, Jacob D, Truc JB, *et al.* Vesicouterine fistulas: Imaging findings in three cases. *AJR Am J Roentgenol* 2005;184:139-42.
45. Magri J. An unusual case of uterovesical fistula. *Br J Surg* 1960;48:69-72.
46. Youssef AF. Menouria following lower segment cesarean section; a syndrome. *Am J Obstet Gynecol* 1957;73:759-67.
47. Body JJ, Acklin YP, Gunther O, Hechmati G, Pereira J, Maniadakis N, *et al.* Pathologic fracture and healthcare resource utilisation: A retrospective study in eight European countries. *J Bone Oncol* 2016;5:185-93.
48. Shon IH, Fogelman I. F-18 FDG positron emission tomography and benign fractures. *Clin Nucl Med* 2003;28:171-5.
49. Shin DS, Shon OJ, Byun SJ, Choi JH, Chun KA, Cho IH, *et al.* Differentiation between malignant and benign pathologic fractures with F-18-fluoro-2-deoxy-D-glucose positron emission tomography/computed tomography. *Skeletal Radiol* 2008;37:415-21.
50. Choi HS, Yoo IeR, Park HL, Choi EK, Kim SH, Lee WH, *et al.* Role of <sup>18</sup>F-FDG PET/CT in differentiation of a benign lesion and metastasis on the ribs of cancer patients. *Clin Imaging* 2014;38:109-14.
51. Jawad MU, Scully SP. In brief: Classifications in brief: Mirels' classification: Metastatic disease in long bones and impending pathologic fracture. *Clin Orthop Relat Res* 2010;468:2825-7.
52. Salavati A, Shah V, Wang ZJ, Yeh BM, Costouros NG, Coakley FV, *et al.* F-18 FDG PET/CT findings in postradiation pelvic insufficiency fracture. *Clin Imaging* 2011;35:139-42.
53. Long NM, Smith CS. Causes and imaging features of false positives and false negatives on F-PET/CT in oncologic imaging. *Insights Imaging* 2011;2:679-98.
54. Tsuchida T, Kosaka N, Sugimoto K, Itoh H. Sacral insufficiency fracture detected by FDG-PET/CT: Report of 2 cases. *Ann Nucl Med* 2006;20:445-8.
55. Iyer R, Jhingran A. Radiation injury: Imaging findings in the chest, abdomen and pelvis after therapeutic radiation. *Cancer Imaging* 2006;6:S131-9.
56. Sahgal A, Whyne CM, Ma L, Larson DA, Fehlings MG. Vertebral compression fracture after stereotactic body radiotherapy for spinal metastases. *Lancet Oncol* 2013;14:e310-20.
57. Burr DB. The contribution of the organic matrix to bone's material properties. *Bone* 2002;31:8-11.
58. Guise TA. Molecular mechanisms of osteolytic bone metastases. *Cancer* 2000;88:2892-8.
59. Hamilton JD, Lai SY, Ginsberg LE. Superimposed infection in mandibular osteoradionecrosis: Diagnosis and outcomes. *J Comput Assist Tomogr* 2012;36:725-31.
60. Alhilali L, Reynolds AR, Fakhra S. Osteoradionecrosis after radiation therapy for head and neck cancer: Differentiation from recurrent disease with CT and PET/CT imaging. *AJNR Am J Neuroradiol* 2014;35:1405-11.
61. Støre G, Boysen M. Mandibular osteoradionecrosis: Clinical behaviour and diagnostic aspects. *Clin Otolaryngol Allied Sci* 2000;25:378-84.
62. Catalano L, Del Vecchio S, Petruzzello F, Fonti R, Salvatore B, Martorelli C, *et al.* Sestamibi and FDG-PET scans to support diagnosis of jaw osteonecrosis. *Ann Hematol* 2007;86:415-23.
63. Welsh JS, Torre TG, DeWeese TL, O'Reilly S. Radiation myositis. *Ann Oncol* 1999;10:1105-8.
64. Floreczynski MM, Sanatani MS, Mai L, Fisher B, Moulin DE, Cao J, *et al.* Severe myositis of the hip flexors after pre-operative chemoradiation therapy for locally advanced rectal cancer: Case report. *BMC Cancer* 2016;16:243.
65. Hird AE, Wilson J, Symons S, Sinclair E, Davis M, Chow E,

- et al.* Radiation recall dermatitis: Case report and review of the literature. *Curr Oncol* 2008;15:53-62.
66. Eckardt MA, Bean A, Selch MT, Federman N. A child with gemcitabine-induced severe radiation recall myositis resulting in a compartment syndrome. *J Pediatr Hematol Oncol* 2013;35:156-61.
67. Fakih MG. Gemcitabine-induced rectus abdominus radiation recall. *JOP* 2006;7:306-10.
68. Agrawal K, Bhattacharya A, Harisankar CN, Abrar ML, Mittal BR, Tripathy SK, *et al.* [18F]Fluoride and [18F] fluorodeoxyglucose PET/CT in myositis ossificans of the forearm. *Eur J Nucl Med Mol Imaging* 2011;38:1956.
69. Al-Nahhas A, Jawad AS. PET/CT imaging in inflammatory myopathies. *Ann N Y Acad Sci* 2011;1228:39-45.